Journal of Catalysis **193,** 58–64 (2000)
doi:10.1006/jcat.2000.2876, available online at http://www.idealibrary.com on IDEAL®

Oxygen Permeation and Oxidative Coupling of Methane in Yttria Doped Bismuth Oxide Membrane Reactor

Y. Zeng and Y. S. Lin[1]

Department of Chemical Engineering, University of Cincinnati, Cincinnati, Ohio 45221-0171

Received September 7, 1999; revised February 29, 2000; accepted March 20, 2000

Disk-shaped dense membranes made of 25 mol% yttria doped bismuth oxide (BY25) in the fluorite-type fcc phase structure (δ-Bi_2O_3 phase) were fabricated by using press/sinter method from the citrate-derived BY25 powders. Oxygen permeation fluxes through these membranes were measured at different temperatures and oxygen partial pressures. The bulk-diffusion is the rate-limiting step for oxygen permeation through a 1.4-mm BY25 membrane with activation energy of about 70 kJ/mol and exponent of 0.25 for oxygen partial pressure dependency. C_2 ($C_2H_4 + C_2H_6$) selectivity and yield achieved for oxidative coupling of methane (OCM) in the BY25 membrane reactor were, respectively, in the range of 20–90% and 16–4%. At the same C_2 yield, the membrane reactor gives C_2 selectivity of about 30% higher than the cofeed fixed-bed reactor packed with BY25 pellets under similar conditions. After OCM the BY25 membrane remained in good integrity but the reaction caused formation of some impurity phases on the membrane surface exposed to the methane stream. © 2000 Academic Press

INTRODUCTION

There was an intensive research effort during the 1980s and early 1990s on direct conversion of natural gas (mainly methane) into value added C_2 ($C_2H_4 + C_2H_6$) product through catalytically oxidative coupling of methane (OCM) (1–4). However, this attempt failed to attract much industrial interest due to low C_2 yield achieved (<30%) when C_2 selectivity was higher than 50%. Most reported studies were carried out in a conventional packed-bed reactor with the cofeed operation mode, i.e., methane and oxygen (or air) were fed together into the reactor. In this case, complete oxidation reaction is often more selective than C_2 formation reactions at high methane conversion due to the existence of molecular oxygen in the gas phase.

In recent years, some research efforts have been directed toward searching for other reactor configurations which would better fit the mechanism of OCM than the packed-bed reactor. Due to their several unique properties, ceramic membrane reactors offer the potential for achieving higher C_2 yield and selectivity (5, 6). Both porous (7, 8) and dense (9, 10) ceramic membranes have been studied for OCM reactions. When a dense oxygen ionic-conducting ceramic membrane is applied, oxygen and methane are, respectively, fed into two chambers separated by the membrane. Oxygen permeates through the membrane by dissociation and bulk diffusion and reacts with methane on the other surface of the membrane. Gas phase oxygen can be greatly minimized or eliminated by matching the oxygen permeation flux with the OCM reaction rate. Therefore, high C_2 selectivity can be expected (9, 10).

A suitable dense oxygen-conducting ceramic membrane should possess both high oxygen permeability and good OCM catalytic properties. Our previous study showed that fluorite-structured 25 mol% Y_2O_3 doped Bi_2O_3 (BY25), an oxygen-ionic-conducting ceramic, exhibited good OCM catalytic properties: C_2 yield of 18% and C_2 selectivity close to 50% in a cofeed packed-bed reactor (oxygen and methane were fed together), and C_2 selectivity as high as 93% with C_2 yield less than 5% in a cyclic packed-bed reactor (oxygen and methane were fed alternatively) (11, 12). The study also showed that the C_2 selectivity of BY25 in the cofeed reactor was lower than 65% even at very small methane conversion, e.g., less than 5%. The higher C_2 selectivity of BY25 in a cyclic packed-bed with essentially no gas phase oxygen present during OCM suggests that the lattice oxygen anions in BY25 are responsible for the formation of C_2 products. On the other hand, the lower C_2 selectivity of BY25 in the cofeed packed-bed reactor with abundant gas phase oxygen molecules present supports the fact that combustion reactions are promoted by the molecular oxygen.

It is known that C_2 yield is mainly related to the amount of lattice oxygen anions available on the surface of BY25 particles. In the cofeed packed-bed reactor, due to the presence of a sufficient amount of oxygen in the gas phase, a high concentration of lattice oxygen anion on the BY25 solid surface can be maintained despite continuous consumption of O^{2-} by OCM reactions. This is warranted by the equilibrium reactions: $O_2(g) <=> O_2(s) <=> 2O^{2-}$ (s) (13). Because of this mechanism, C_2 yield in the cofeed packed-bed reactor is much higher than that in the cyclic packed-bed reactor.

---

[1] To whom correspondence should be addressed.

0021-9517/00 $35.00

For the latter reactor there is no means to instantaneously renew those consumed lattice oxygen anions.

The dense oxygen semipermeable membrane reactor for OCM combines advantages of both cofeed and cyclic pack-bed reactors and avoids their disadvantages (14, 15). In this type of reactor, the elimination of gas phase oxygen molecules is achieved by using a dense membrane which separates the feedings of methane and oxygen. The concentration of the lattice oxygen anions on the membrane surface exposed to methane is maintained through the continuous flow of oxygen anions from the oxygen feed side to the reaction side. According to this mechanism, it is expected that the OCM dense membrane reactor is able to achieve both high C_2 yield and selectivity. As mentioned before, a suitable dense membrane for OCM membrane reactor must possess: (1) good OCM catalytic properties; (2) high oxygen semipermeability in the OCM reaction temperature range, i.e., 700–1000°C; and (3) good chemical, phase structural, and mechanical stability during application.

According to our previous study BY25 membrane seems to fulfill the first requirement, i.e., possession of good OCM catalytic properties. In this study, we examined OCM performance in the membrane reactor made of BY25. The oxygen permeation through the membranes as well as its stability is also reported in this paper.

EXPERIMENTAL

Powders of BY25 oxides were prepared by the citrate method. In this method, stoichiometric amounts of the corresponding metal nitrates, i.e., $Bi(NO_3)_3 5H_2O$ (99%, Fisher), $Y(NO_3)_3 \cdot 6H_2O$ (99.5%, Alpha), were fully dissolved in a dilute nitric acid solution (at DI water to concentrated HNO_3 volume ratio of 9 to 1), followed by addition of citric acid (99%, Fisher). The molar amount of the citric acid was 1.5 times that of the total metal ions. Thus obtained solution was heated while stirring to temperature of about 90–110°C. After the system was isothermally refluxed and stirred for 3 h, water was removed through evaporation until a sticky gel-like solid was formed.

The above-mentioned gel was dried at 110°C in a box oven overnight and then placed in a box furnace preheated to 400°C. The sample was ignited at a temperature of around 350°C and formed a fine powder which was further calcined at 600°C for 3–5 h to obtain a yellowish powder, here referred to as green (unsintered) powder of BY25 oxides. In order to make disk-shaped BY25 membranes, the green powders were packed in a stainless steel mold (26.5 mm in diameter) and isostatically pressed into disks by imposing a hydraulic pressure of 120 MPa. The green disks were then sintered at 1000°C in air for 48 h.

Oxygen permeation measurement and OCM reactions were conducted in a home-made high-temperature oxygen permeation cell. The detailed description of this system is given elsewhere (16). A BY25 disk-shaped membrane with 21 mm diameter and 1.4 mm thickness was sealed onto the top of an alumina tube with a Bi_2O_3-based sealant made of a mixture of BY25 and silica powders. This sealant was pasted and became gas-tight when temperature reached 700–850°C. The gas tightness of this sealant usually lasted for 1–3 days. During permeation measurements the membrane was exposed to the streams of oxygen/nitrogen mixture (feed side) and pure helium (permeate side). Helium flow rate on the permeate side was 50 ml/min, and the total flow rate on the feed side was controlled in 30–60 ml/min. It was found that the feed side flow rate had little effect on the oxygen permeation flux.

For OCM reaction, the membrane was exposed to the streams of methane/helium (10 : 90) mixture (methane side) and oxygen/nitrogen (50 : 50) mixture (oxygen side). During the experiments, the oxygen side feed flow was controlled at 50 ml/min while the methane side feed flow was varied from 60 to 220 ml/min. The reactions took place at the atmospheric pressure. Typically, the applied sealant was able to maintain gas-tightness up to 9 h under OCM reaction conditions.

The compositions of the effluents from the permeation cell were analyzed by gas chromatography. Leakage of gas through the sealant, if occurred, was detected by observing nitrogen in the effluent of the permeate side (helium or methane/helium stream). Phase structures of BY25 membranes before and after oxygen permeation measurement and OCM reaction were examined by X-ray diffraction (Siemens Kristalloflex D500 diffractometer, with Cu $K\alpha$ radiation). The detailed experimental procedures for oxygen permeation, OCM reactions, and characterization can be found in our previous publication on OCM in a perovskite-type ceramic membrane reactor (16).

RESULTS AND DISCUSSION

Oxygen Permeation

Figure 1 shows oxygen permeation flux through a 1.4-mm thick BY25 membrane in 750–950°C. The oxygen partial pressures of the upstream and downstream on each side of the membrane, P_{high}, P_{low}, were, respectively, 0.36 and 0.002 atm. As shown, oxygen permeation flux increases substantially with increasing temperature. An Arrhenius plot of J_{O_2} against $1/T$, as shown in Fig. 1b, gives an apparent activation energy of 70.2 kJ/mol with a preexponential constant of 2.02×10^{-5} mol/cm^2/s.

Figures 2a and 2b, respectively, show the oxygen permeation flux at 950°C as a function of P_{high} and P_{low}. It shows that the flux increases with increasing oxygen partial pressure in the upstream chamber while decreases with increasing oxygen partial pressure in the downstream chamber. This can be easily explained by the fact that the driving force

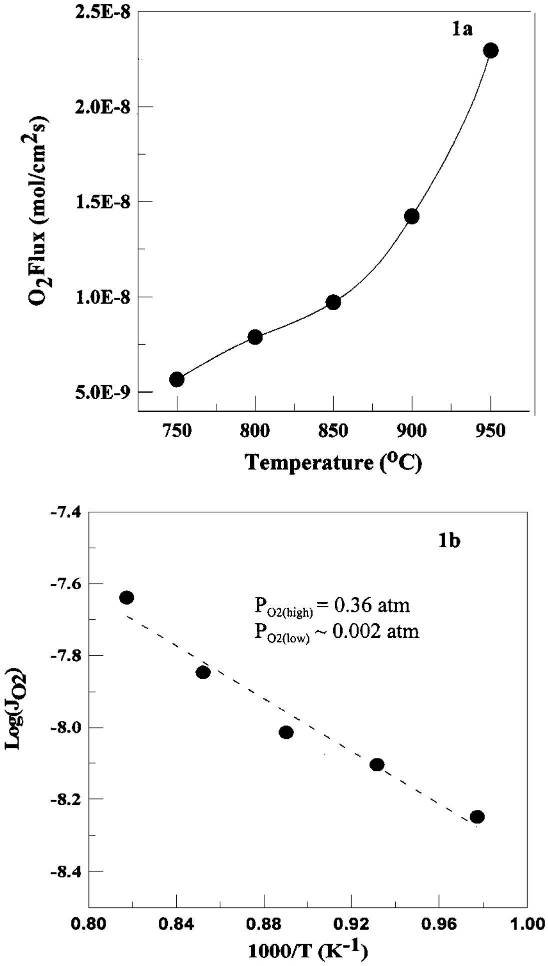

FIG. 1. Temperature dependence of oxygen permeation flux through BY25.

for oxygen permeation through the membrane increases with increasing P_{high} and decreasing P_{low}. The two sets of the permeation data shown in Fig. 2 can be well correlated by

$$J_{O_2} = k\left[P_{\text{high}}^{1/4} - P_{\text{low}}^{1/4}\right] \quad [1]$$

with the same value of $k = 4.4 \times 10^{-8}$ mol/cm^2/s for both sets of the data, as shown in Fig. 3. Lin *et al.* (17) showed that the oxygen permeation through zirconia or bismuth oxide based ionic conducting ceramic membranes can be described by

$$J_{O_2} = \alpha\left[P_{\text{high}}^{\frac{1}{2}} - P_{O_2(\text{I})}^{\frac{1}{2}}\right] \quad [2]$$

$$J_{O_2} = \frac{\beta}{L}\left[P_{O_2(\text{I})}^{1/4} - P_{O_2(\text{II})}^{1/4}\right] \quad [3]$$

$$J_{O_2} = \alpha\left[P_{O_2(\text{II})}^{\frac{1}{2}} - P_{\text{low}}^{\frac{1}{2}}\right], \quad [4]$$

where L is the membrane thickness, α is the rate constant related to the surface adsorption and charge transfer reactions, β is related to the electron-hole conductivity at the standard conditions (17), and, $P_{O_2(\text{I})}$ and $P_{O_2(\text{II})}$ are, respectively, hypothetical oxygen partial pressures equilibrated with the electron-hole concentrations on the membrane surfaces of the upstream and downstream sides. If the bulk diffusion is the rate-limiting step $[(\beta/L) \ll \alpha]$, Eqs. [2]–[4] can be simplified to Eq. [1] with $k = (\beta/L)$. The good agreement between the experimental data and Eq. [1] as shown in Fig. 3 suggests that the oxygen permeation through the 1.4 mm thick BY25 membrane at 950°C is rate-limited by the bulk-diffusion process, i.e., the transportation of electron holes across the membrane.

There has been no data reported on oxygen permeation through yttria doped bismuth oxide membranes. Bouwmeester *et al.* (18) studied oxygen semipermeability of 25% erbia doped bismuth oxide (BE25) membrane. They observed that the apparent kinetic order for oxygen permeation through the BE25 membrane at 810°C increased

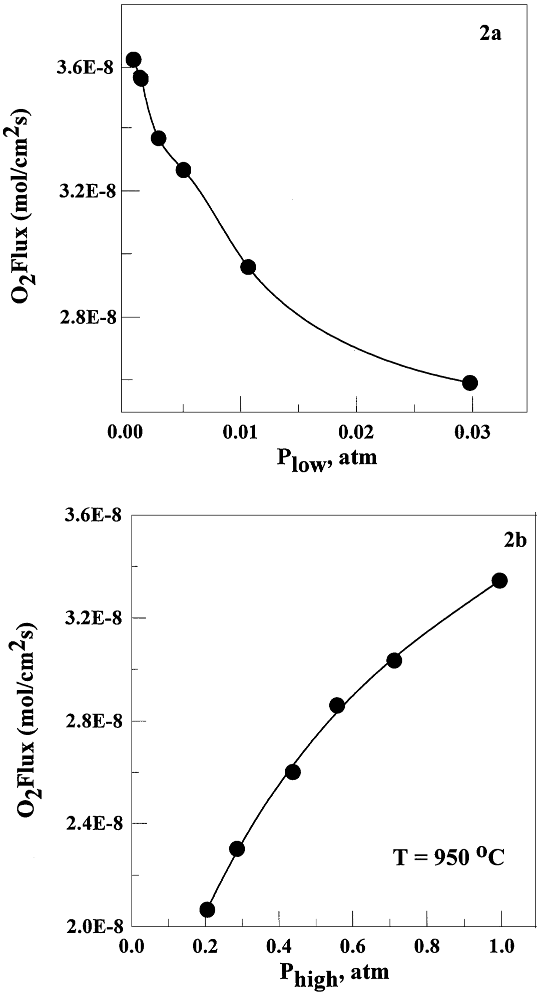

FIG. 2. Pressure dependence of the oxygen permeation flux through BY25.

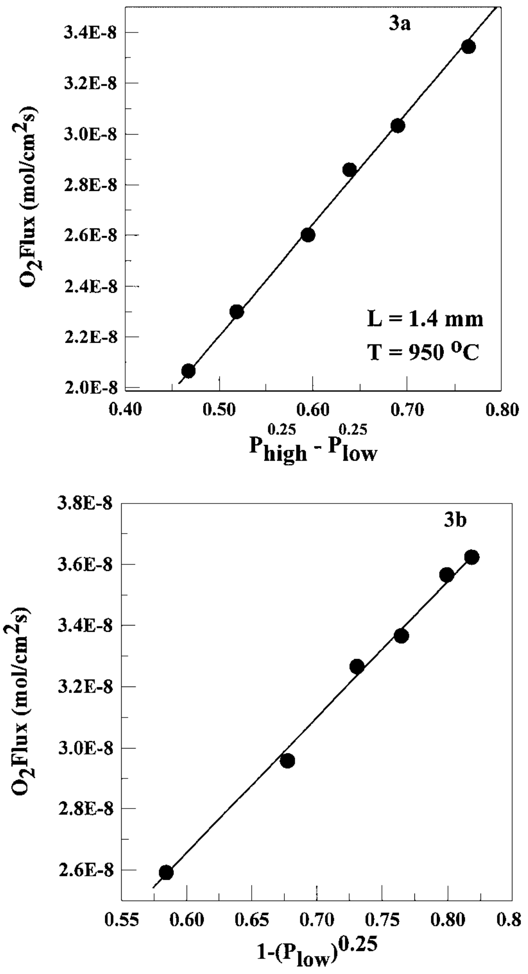

FIG. 3. Regression of oxygen permeation data with Eq. [1] (3a-varying P_{high} and P_{low}: 3b-varying P_{low} at fixed $P_{high} = 1$ atm; pressures are given in the unit of atm.

from 0.37 to 0.52 when membrane thickness decreased from 2.85 mm to 0.2 mm, indicating that the rate-limiting step shifts from the bulk diffusion toward the surface reaction as the membrane becomes tinner. These results can be described by Eqs. [2]–[4]. They also found that the activation energies for bulk diffusion and surface reaction were, respectively, 99 and 136 kJ/mol. The activation energy observed in this study for BY25 is lower than that for the bulk diffusion in BE25 membranes.

The activation energy for surface reaction is generally higher than that for bulk diffusion. Therefore, the latter is more likely to become rate-limiting at higher temperatures, e.g., 950°C, in our study. With the bulk diffusion as the rate-limiting step, the oxygen permeation flux through a 0.7 mm thick BY25 membrane under oxygen pressure gradient of $P_{high} = 1$ atm and $P_{low} = 1.1 \times 10^{-4}$ atm at 810°C is calculated to be 2.7×10^{-8} mol/cm^2/s according to Eq. (1). This flux is about 4 times that of BE25 under the identical conditions (6.7×10^{-9} mol/cm^2/s) reported by Bouwmeester *et al.* (18). The higher oxygen permeation flux for the BY25 membrane as compared to the BE25 membrane is consistent with the lower activation energy observed for the former. The oxygen permeation flux in these two membranes is proportional to the electronic conductivity of BY25 or BE25, which is determined by the band gap energy for electron transport. Thus the present results indicate a lower band gap energy for yttria doped bismuth oxide than the erbia doped bismuth oxide.

OCM in BY25 Membrane Reactor

During OCM reactions there was essentially no oxygen leaking through the sealant for the experiment period of about 9–10 h. Neither oxygen nor CO was detected in the effluent of the product stream. Figures 4–7 show the temperature dependence of CH_4 conversion, C_2 selectivity, C_2 yield and C_2H_4/C_2H_6 ratio in C_2 products for OCM in the BY25 membrane reactor. As shown in Fig. 4, CH_4 conversion increases exponentially with increasing temperature. This can be explained by the following mechanisms.

When the BY25 membrane is employed in the OCM membrane reactor, reactions on the membrane surface exposed to methane may be described by the paths

$$CH_4(g) \Leftrightarrow CH_4(s) \qquad [A]$$

$$CH_4(s) + \frac{1}{2}O_O^x + h^{\cdot} \Leftrightarrow CH_3\cdot + \frac{1}{2}H_2O \qquad [B]$$

$$2CH_3\cdot \rightarrow C_2H_6. \qquad [C]$$

Since reaction (C) is a fast irreversible reaction, the net oxygen flux through the interface at the methane side is determined by adsorption–desorption equilibrium of methane onto the solid phase and the supply of electron-holes from

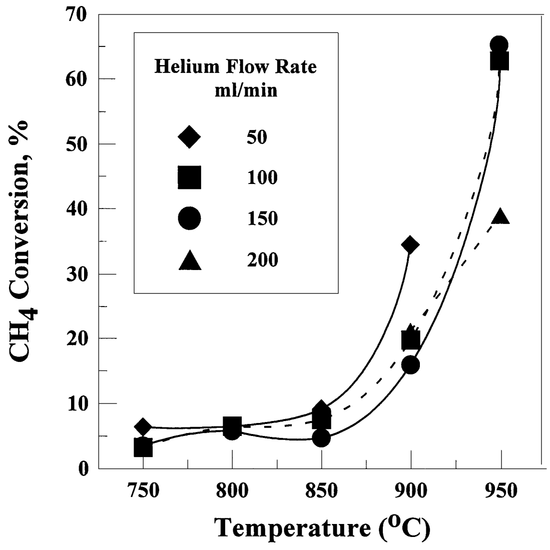

FIG. 4. Methane conversion as a function of temperature in BY25 membrane reactor.

the other side of the membrane. The reaction on the other membrane surface occurs as

$$O_{2,g} + 2V_O^{\cdot\cdot} \Leftrightarrow 2O_O^x + 4h^{\cdot}. \qquad [D]$$

The above analysis suggests that the formation rate of ethane is determined by the concentration of methane in the gas phase and the concentration of the electron-holes in the solid phase on the membrane surface exposed to methane

$$r_{C_2H_6} = k_{C_2H_6}[CH_4]p'', \qquad [5]$$

where $k_{C_2H_6} = k_A k_B [O_O^x]^{\frac{1}{2}}$, and P'' is the electron-hole concentration on the membrane surface exposed to methane stream. k_A and k_B are forward rate constants for reactions [A] and [B]. Thus, ethane formation rate in a membrane reactor can be enhanced by raising concentrations of methane and electron-holes on the membrane surface. Since methane concentration in the gas phase is almost constant in the present experiments, the reaction rate is primarily determined by electron-hole transfer rate, i.e., oxygen permeation rate through the membrane. As shown in the previous section, the permeation rate increases exponentially with increasing temperature. Therefore, the reactivity of the membrance surface for OCM also increases exponentially with the temperature, as shown in Fig. 4.

In the membrane reactor, C_2 selectivity decreases with increasing temperature in 750–950°C, as shown in Fig. 5. For comparison, Fig. 8 shows C_2 selectivity and yield on BY25 pellets packed in a cofeed fixed-bed reactor. These dense BY25 pellets were 1–3 mm in size and prepared by cracking the same BY25 membrane used in this work. OCM reactions were conducted on the fixed-bed packed with 0.6 g of the BY25 pellets. The feed was a mixture of methane/oxygen/helium (2.9 : 1 : 1.3) at a total feed flow rate of 99 ml/min, as detailed elsewhere (11). As shown in Fig. 8, in the fixed-bed reactor the C_2 selectivity increases, up to 900°C, and then decreases with increasing temperature.

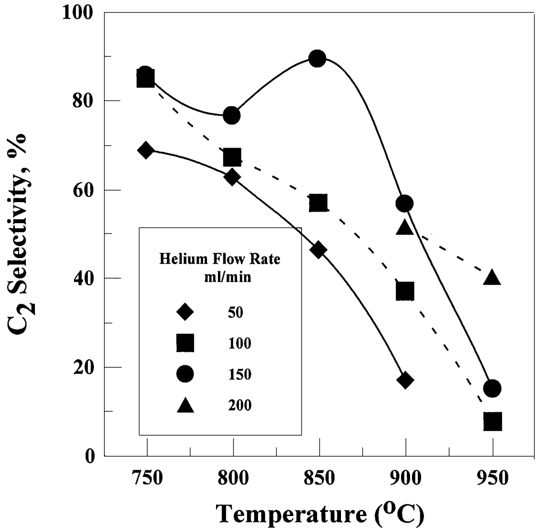

FIG. 5. C_2 selectivity as a function of temperature in the BY25 membrane reactor.

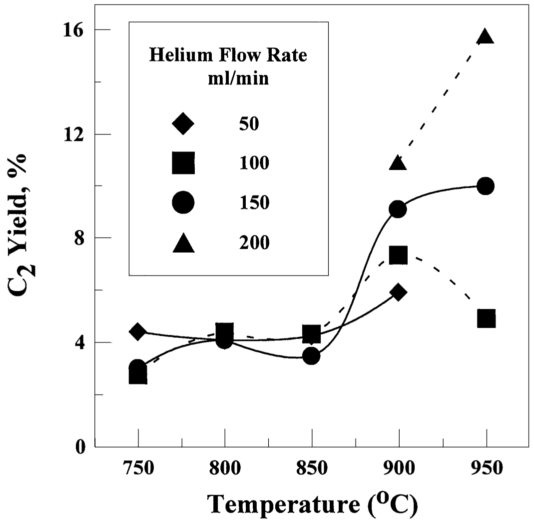

FIG. 6. C_2 yield conversion as a function of temperature in the BY25 membrane reactor.

At temperatures lower than 900°C the C_2 selectivity increases with temperature. This could be due to the stronger temperature dependency of oxygen permeation flux as compared with the C_2 formation rate in this temperature range under the membrane reactor conditions. In this case more oxygen slips into the gas phase as temperature increases, thus lowering the C_2 selectivity. This is consistent with the simulation results (14). The dramatic decrease in C_2 selectivity in the membrane reactor at temperatures higher than 900°C could be a result of the combined effects of the excessive amount of oxygen present in the gas phase and dramatic decrease in the selectivity of the BY25 material surface.

As shown in Fig. 6, C_2 yields are maintained around 4% in the temperature range of 750–850°C and increase drastically from 850 to 900°C. They then level off or decrease as temperature further increases from 900 to 950°C. Comparing the C_2 yield and selectivity data shown in Figs. 5, 6, and 8, it is clear that at the same yield (<5%) (at around 850°C), the C_2 selectivity in the membrane reactor is about 80% (Fig. 5), in contrast to about 50% for the cofeed fixed-bed reactor. This indicates that in the membrane reactor the gas phase oxygen in the methane side is substantially minimized and thus the C_2 selectivity is improved.

The C_2 yields obtained in the membrane reactor were in the range of 2–9%. These are lower than that obtained in the fixed-bed reactor packed with finer BY25 particles (about 18%) (11), but close to that packed with the large BY25 pellets shown in Fig. 8. This is due to the fact that in the current membrane reactor configuration only a portion of methane was actually brought into contact with the surface

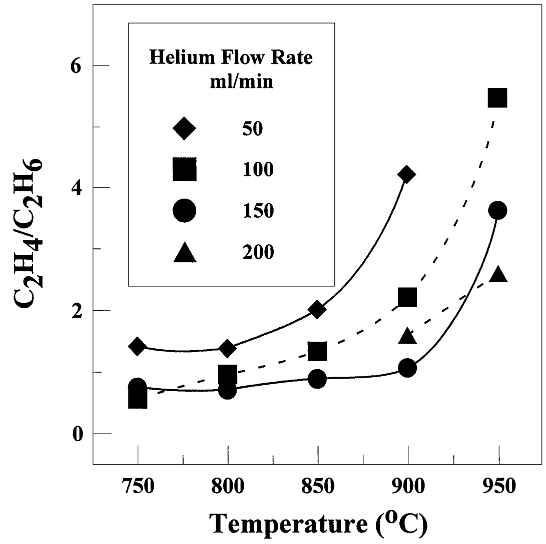

FIG. 7. C_2H_4/C_2H_6 ratio as function of temperature in the BY25 membrane reactor.

of BY25 disk and participated in OCM reactions with the solid phase oxygen, i.e., O^{2-}. This problem could be solved by using a membrane reactor with a large surface area to volume ratio (such a smaller membrane tubes). Nevertheless, C_2 yield achieved in this work was higher than that reported on OCM in dense ceramic membrane reactors of the same configuration (<3%) (9, 10) due to a much higher OCM reactivity of BY25 as compared to many other catalysts studied for OCM (11).

Figure 7 shows the effect of temperature on C_2H_4/C_2H_6 ratio in C_2 products. As shown, C_2H_4/C_2H_6 ratio increases exponentially with increasing temperature. Since ethylene is more useful than ethane, it is quite encouraging to see that C_2H_4/C_2H_6 ratio as high as 4 was achieved in the BY25 membrane reactor. In the OCM catalytic reactions, ethylene is believed to be derived from ethane with the reactions

$$C_2H_6(g) \Leftrightarrow C_2H_6(s) \qquad [D]$$

$$C_2H_6(s) + O_O^x + 2h^{\cdot} \Leftrightarrow C_2H_4 + H_2O \qquad [E]$$

and its formation rate can be described by

$$r_{C_2H_4} = k_{C_2H_4}[C_2H_6]p''^2, \qquad [6]$$

where $k_{C_2H_4} = k_D k_E [O_O^x]$, k_D and k_E are forward rate constants for reactions [D] and [E]. At constant temperature and partial pressures for oxygen and methane, OCM reactions in the BY25 membrane reactor could be considered as a steady-state process. Thus, from Eqs. [5] and [6], C_2H_4/C_2H_6 ratio can be expressed by

$$C_2H_4/C_2H_6 = \frac{k_{C_2H_4}}{k_{C_2H_6}}\frac{[C_2H_6]p''}{[CH_4]}. \qquad [7]$$

The reaction rate constants are correlated exponentially to the activation energies for Reactions [A] and [B], and [D] and [E]. The results given in Fig. 7 suggest that the activation energies for the reactions [D] and [E] are larger than those for reactions [A] and [B].

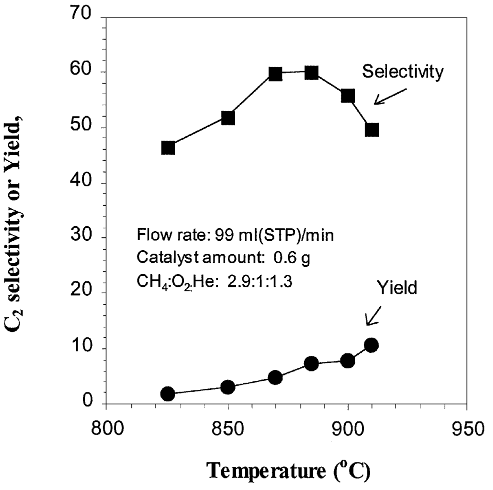

FIG. 8. C_2 selectivity and yield on cofeed fixed-bed reactor packed with BY25 pellets (conditions given in text).

The effect of total flow rate (in the reaction chamber) on the OCM performance of BY25 membrane reactor is also illustrated in Figs. 4–7. It is clear that C_2 selectivity increases with increasing flow rate. This is consistent with the fact that a higher flow rate facilitates mass transfer in the reactor. The C_2H_4/C_2H_6 ratio decreases with increasing flow rate since C_2H_6 is less likely to be further oxidized into C_2H_4 as residence time decreases. It is interesting to see that neither CH_4 conversion nor C_2 yield decreases significantly, as expected, with increasing flow rate. In contrast, a linear increase in the C_2 yield with flow rate is observed at 900°C.

Oxygen permeation rate during OCM at 800°C and helium flow rate 50 ml/min (5 ml/ml methane flow rate) was calculated to be 8.6×10^{-8} mol/cm^2/s from the data of flow rates, methane conversion and selectivity. This rate is larger than the oxygen permeation flux with pure helium as the purge gas under similar conditions. This difference is due, at least in part, to the larger oxygen partial pressure gradient during OCM reaction ($P_{high} = 0.5$ atm, $P_{low} < 10^{-8}$ atm) than that during the oxygen permeation experiments, according to Eq. [1].

The methane turn over frequency (TOF) was roughly estimated assuming that the oxygen vacancy is the active site and there are 2 oxygen vacancies in each unit cell of BY25 (three Bi^{3+}, one Y^{3+}, six O^{2-}). The total number of active sizes was calculated from the lattice parameter of BY25 (0.555 nm) and the membrane surface area. At 900°C the TOF is estimated at the range of 140–625 1/s in the helium flow rate of 50–150 ml/min. TOF increases with increasing temperature and flow rate.

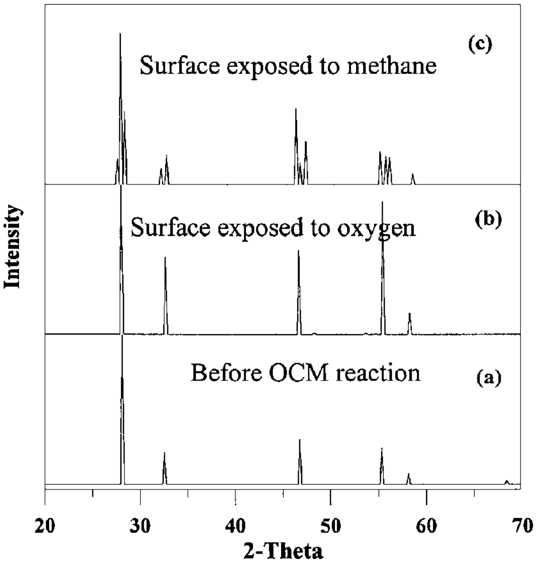

FIG. 9. XRD patterns of BY25 membrane (a) before and (b) and (c) after OCM.

The BY25 membranes after OCM reactions still remained in good integrity. It is known that bismuth oxide is thermodynamically much less stable than zirconia in the reducing atmosphere. However, our recent cyclic study (19) shows that bismuth or yttrium ion in BY25 remains unreduced in the methane/helium atmosphere during OCM reaction as long as the stoichiometric oxygen in BY25 has not been consumed. Figure 9 shows the XRD patterns of BY25 membrane before and after the OCM reactions. The XRD pattern before the reactions shows a perfect fcc phase structure. After OCM reactions, the surface exposed to oxygen still remains in the fcc phase structure. The surface exposed to methane stream exhibits several new XRD peaks in addition to those of the fcc phase. This indicates that the majority of the BY25 membrane remains unreduced after the prolonged OCM experiments. Therefore, a continuous supply of the oxygen for the BY25 when operated in the membrane mode has prevented full reduction of metal ions in the BY25 membrane with one surface exposed to methane.

CONCLUSIONS

Oxygen permeation flux through BY25 membrane is around 1.0×10^{-8} mol/cm^2/s at 850° with an activation energy of about 70 kJ/mol. The oxygen pressure dependency of permeation flux follows the power law with the exponent of 0.25 on oxygen partial pressure. Bulk diffusion of the electron-holes is the rate-limiting step for oxygen permeation. Much higher C_2 selectivity (about 80%) is obtained for OCM in the BY25 membrane reactor than in the cofeed reactor packed with the pellets of the same BY25 (about 50%) at the same C_2 yield (about 5%). The results show that the membrane reactor is effective in improving C_2 selectivity. The stability of the membrane material and reactor configuration of the membrane reactor should be improved in order to demonstrate more promising results of OCM on this type of membrane reactor.

ACKNOWLEDGMENT

This project was supported by the National Science Foundation (CTS-9502437, Career Award). Y. Zeng acknowledges the support from Quantum Chemical Corporation in the form of a Graduate Fellowship.

REFERENCES

1. Lee, J. S., and Oyama, S. T., *Catal. Rev. Sci. Eng.* **30**, 249 (1988).
2. Hutchings, G. J., Scurrell, M. S., and Woodhouse, J. R., *Chem. Soc. Rev.* **18**, 251 (1989).
3. Amenomiya, Y., Birss, V. I., Goledzinowski, M., Galuszka, J., and Sanger, A. R., *Catal. Rev. Sci. Eng.* **32**, 163 (1990).
4. Fox, J. M., *Catal. Rev. Sci. Eng.* **35**, 169 (1993).
5. Bouwmeester, H. J. M., and Burggraaf, A. J., in "Fundamentals of Inorganic Membrane Science and Technology" (A. J. Burggraaf and L. Cot, Eds.), Chap. 10. Elsevier, Amsterdam, 1996.
6. Hsieh, H. P., "Inorganic Membranes for Separation and Reaction." Elsevier, Amsterdam, 1996.
7. Lafarga, D., Santamaria, J., and Menendez, M., *Chem. Eng. Sci.* **49**, 2005 (1994).
8. Coronas, J., Menendez, M., and Santamaria, J., *Chem. Eng. Sci.* **49**, 2015 (1994).
9. Xu, S., and Thomson, W. J., *AIChE J.* **43**, 2731 (1997).
10. ten Elshof, J. E., Bouwmeester, H. J. M., and Verweij, H., *Appl. Catal. A* **130**, 195 (1995).
11. Zeng, Y., and Lin, Y. S., *Appl. Catal. A* **159**, 101 (1997).
12. Zeng, Y., and Lin, Y. S., *Ind. Eng. Chem. Res.* **36**, 277 (1997).
13. Maitra, A. M., *Appl. Catal. A: General* **104**, 11 (1993).
14. Wang, W., and Lin, Y. S., *J. Membrane Sci.* **103**, 219 (1995).
15. Kao, Y. K., Lei, L., and Lin, Y. S., *Ind. Eng. Chem. Res.* **36**, 3583 (1997).
16. Zeng, Y., Lin, Y. S., and Swartz, S. L., *J. Membrane Sci.* **150**, 87 (1998).
17. Lin, Y. S., Wang, W., and Han, J., *AIChE J.* **40**, 786 (1994).
18. Bouwmeester, H. J. M., Kruidhof, H., Burggraaf, A. J., and Gellings, P. J., *Solid State Ionics* **53–56**, 460 (1992).
19. Zeng, Y., and Lin, Y. S., *J. Catal.* **182**, 30 (1999).